Electronic Supplementary Material (ESI) for Lab on a Chip

Supplementary Information for "Engineering and Analysis of Surface Interactions in a Microfluidic Herringbone Micromixer"

Thomas P. Forbes and Jason G. Kralj
National Institute of Standards and Technology, Gaithersburg, MD, USA

Table of Contents

Simulation Background

Computational Fluid Dynamics Model

The computational model employed the full Navier-Stokes equations of motion and continuity for determination of the flow profile in a single unit cell of the staggered herringbone geometry. The model solves the following nondimensional set of steady-state incompressible equations for a single liquid phase.

Continuity equation $$\vec{\nabla} \cdot \vec{u} = 0 \quad \text{(S1)}$$

Steady-state Navier-Stokes equations of motion $$\vec{u} \cdot \vec{\nabla}\vec{u} = -\mathrm{Eu}\left[\vec{\nabla}p\right] + \frac{1}{\mathrm{Re}}\left[\vec{\nabla}^2\vec{u}\right] \quad \text{(S2)}$$

Here, the velocity ($\vec{u}$) and pressure (p) are rendered dimensionless by introducing the following dimensionless groups: Euler number ($\mathrm{Eu} = p_o/\rho U^2$) and Reynolds number ($\mathrm{Re} = \rho U D_h/\eta$). In these dimensionless parameters, p_o is the characteristic pressure, ρ is the fluid density, U is the characteristic velocity taken as the linear inlet velocity, $D_h = 4A/P$ is the hydraulic diameter of the main channel, A is the channel cross sectional area, P is the channel perimeter, and η is the dynamic viscosity of the fluid. Given an inlet free stream velocity and no slip and no penetration conditions at all channel walls, the steady-state Navier-Stokes and continuity equations were solved to provide the three-dimensional velocity field. The fluid properties were assumed to be those of water at room temperature, i.e., η = 0.001 kg/m·s and ρ = 1000 kg/m^3. Most molecular and biomolecular surface binding assays utilize similar

Newtonian buffers. A demonstration of the flow profile and velocity field produced by the computational fluid dynamics software ESI-CFD-ACE (Version 2010.0, ESI Group CFD, Paris, France)[1] can be seen in Fig. S1. The simulation domain mesh was variable depending on the overall domain size, but ranged from approximately 4×10^5 nodes for the base case up to 1×10^6 nodes for the larger simulation geometries, i.e., larger herringbone pitch (and overall length), channel height, or herringbone groove depth.

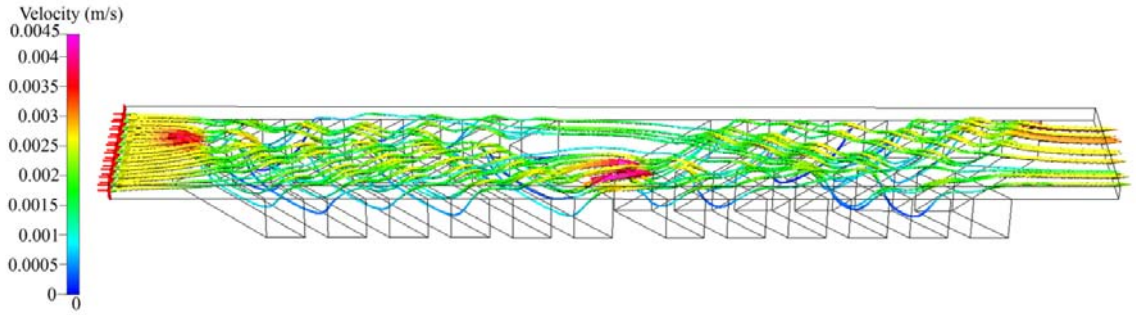

Fig. S1. Simulated flow velocities along a grid of streamlines ($\Delta x = 50$ μm and $\Delta y = 20$ μm) starting at the herringbone unit cell inlet.

Numerical Analysis of Streamlines

For the numerical analysis of surface interactions, a set grid ($\Delta x = \Delta y = 10$ μm) is specified at the inlet for each simulation domain (Fig. S2). The specified grid of streamlines is analyzed using a numerical code in MATLAB (Version R2010a, The Mathworks, Inc., Natick, MA).[2] The locations for which each streamline travels within a particle radius of the domain wall were labeled and recorded. A visual demonstration of the typical output is shown in Fig. S3 for ten streamlines. Surface interactions were broken down by the location of contact.

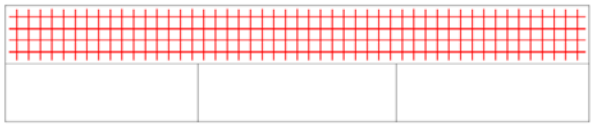

Fig. S2. Uniform grid ($\Delta x = \Delta y = 10$ μm) used to define starting point for an array (49 × 4 in this case) of streamlines at the herringbone unit cell inlet.

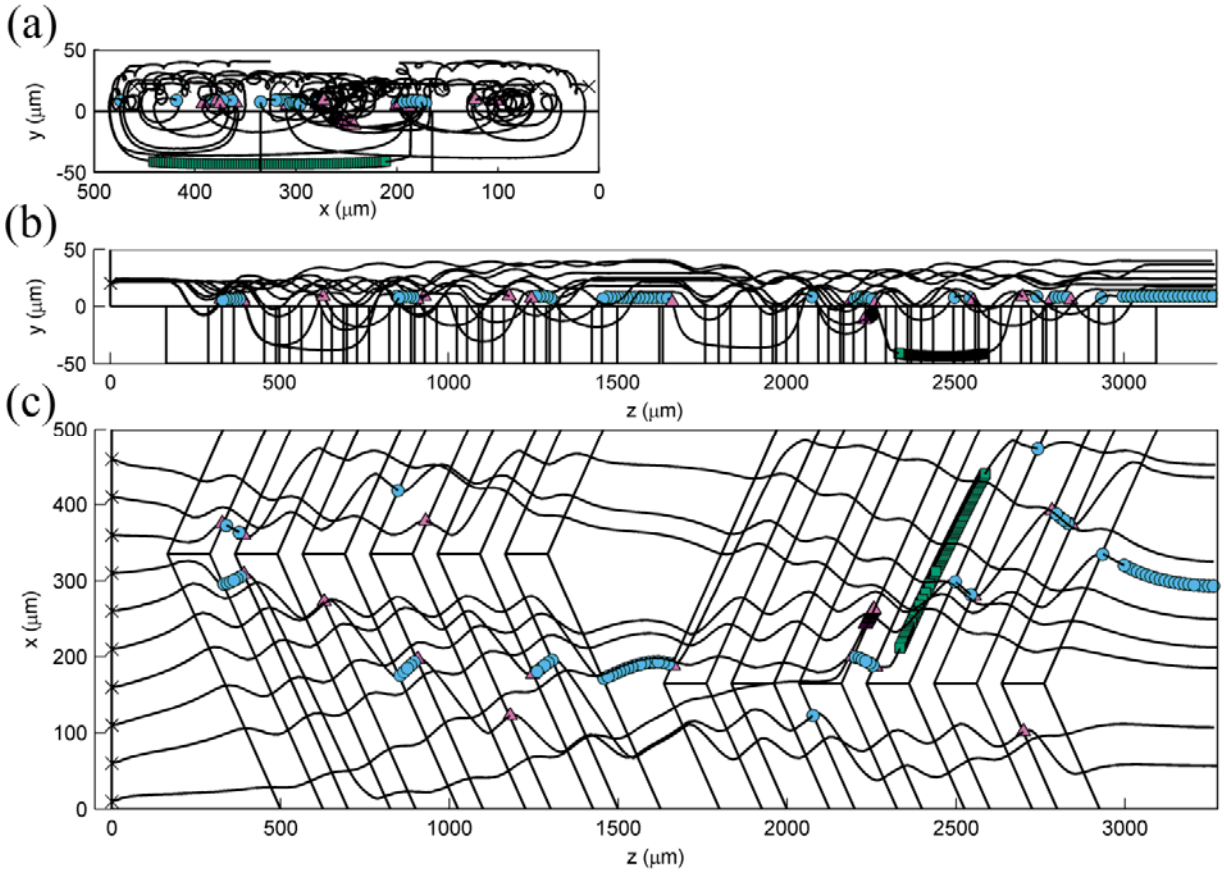

Fig. S3. Representative example of the numerical identification of surface interaction locations at the channel top (♦), channel bottom (●), herringbone groove bottom (■), and herringbone groove sides (▲). (a) Front, (b) side, and (c) top view of the simulated domain.

Numerical Results

Parametric Investigation

The distribution of contact locations as a function of groove width (Fig. 2 and S4), groove depth (Fig. S6), groove pitch (Fig. 3 and S5), channel height (Fig. S7(a)), Reynolds number (Fig. S7(b)), and particle radius (Fig. S8) are displayed below. All other parameters were those of the base case, given in the manuscript text.

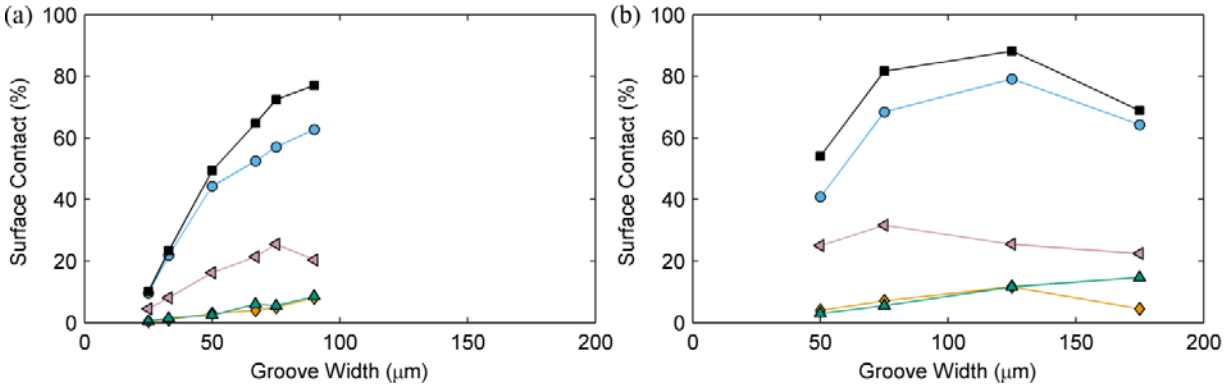

Fig. S4. Simulated surface contact as a function of the herringbone groove width for a (a) 100 μm and (b) 300 μm groove pitch, broken down by contact location. Data are for streamlines in contact with channel top (♦), channel bottom (●), groove bottom (▲), groove sides (◀), and total contact (■).

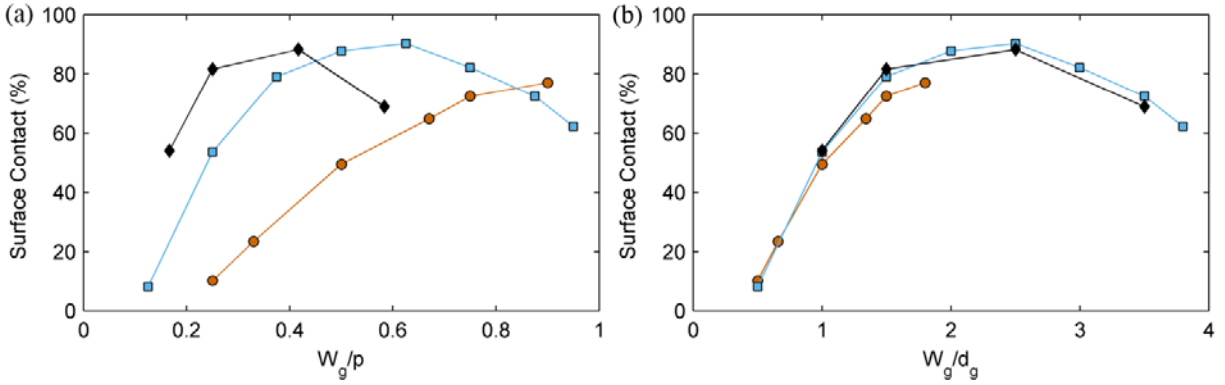

Fig. S5. Simulated surface contact (total) as a function of ratio of (a) groove width to groove pitch and (b) groove width to groove depth (50 μm), for 100 μm (●), 200 μm (■), and 300 μm (♦) groove pitch.

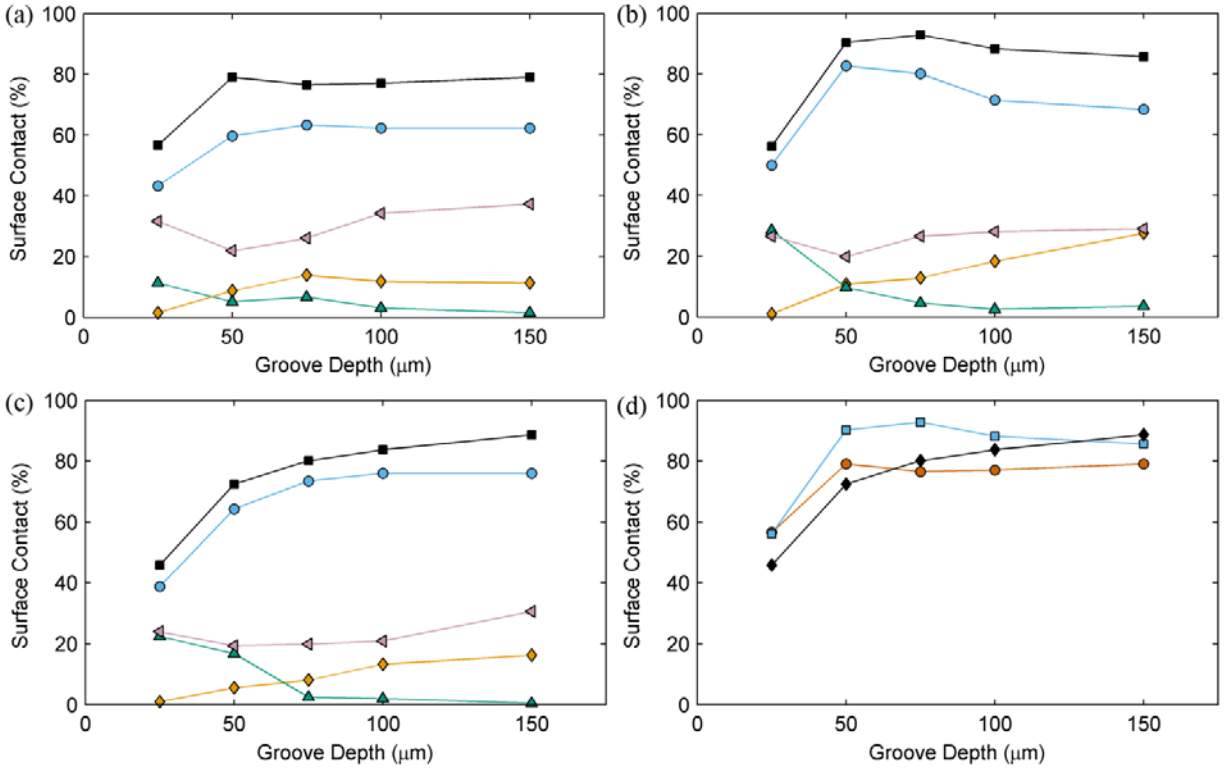

Fig. S6. Simulated surface contact as a function of the herringbone groove depth for a (a) 75 μm, (b) 125 μm, (c) 175 μm groove width and 200 μm groove pitch, broken down by contact location. Data are for streamlines in contact with channel top (♦), channel bottom (●), groove bottom (▲), groove sides (◀), and total contact (■). (d) Simulated surface contact (total) as a function of ratio of groove depth, for 75 μm (●), 125 μm (■), and 175 μm (♦) groove width.

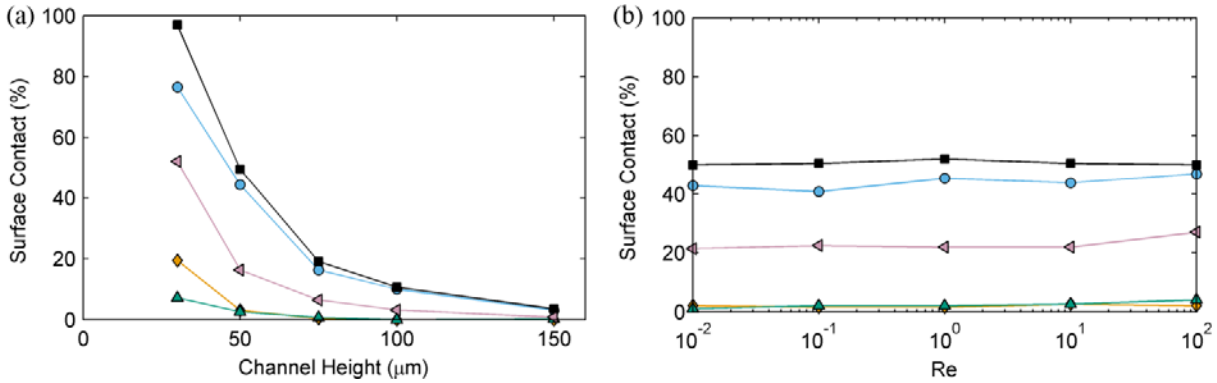

Fig. S7. Simulated surface contact as a function of the (a) channel height and (b) Reynolds number for the base case domain, broken down by contact location. Data are for streamlines in contact with channel top (♦), channel bottom (●), groove bottom (▲), groove sides (◀), and total contact (■).

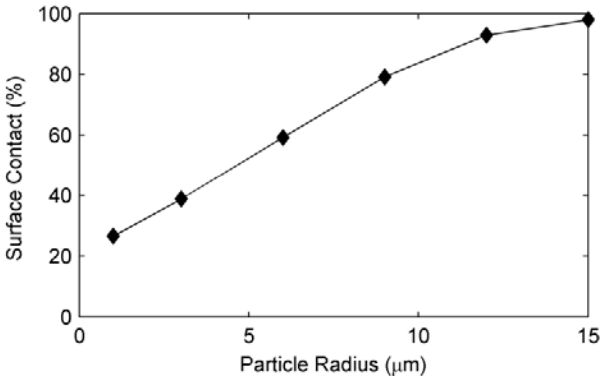

Fig. S8. Simulated surface contact as a function of the particle radius for a 75 μm groove width and 200 μm groove pitch.

Hydraulic Resistance Analysis

As discussed in the manuscript, the complex interplay between flow through the channel and flow within the grooves, and their hydraulic resistances, were identified as the root-causes for the nature of the flow profile for varying groove widths. As given by Kirby 2010,[3] the hydraulic resistance in a rectangular channel is a function of the fluid viscosity (η), channel length (L), hydraulic radius ($R_h = 2A/P = 2wh/(2w + 2h)$) and cross sectional area ($A = wh$).[3]

$$R \approx \frac{8\eta L}{R_h^2 A} \tag{S3}$$

For a given herringbone micromixer geometry and fluid, the hydraulic resistances within a groove and of the channel above the groove can be derived from Equation S3 and are given below.

$$R_{groove} \approx \frac{8\eta L}{R_h^2 A} = \frac{8\eta L_{eff}}{4w_g^3 d_g^3/(2w_g+2d_g)^2} \tag{S4}$$

$$R_{ch} \approx \frac{8\eta L}{R_h^2 A} = \frac{8\eta w_g}{4w_{eff}^3 h^3/(2w_{eff}+2h)^2} \tag{S5}$$

Here, L_{eff} is the effective length of the specific groove, taken as the average groove length, w_g is the groove width, and d_g is the groove depth. The hydraulic radius of the groove is given by, $R_{h(groove)} = 2w_g d_g/(2w_g + 2d_g)$ and the cross sectional area, $A = w_g d_g$. For the channel above a groove, w_{eff} is the

effective width above the groove, h is the channel height, $R_{h(ch)} = 2w_{eff}h/(2w_{eff} + 2h)$ is the hydraulic radius, and $A = w_{eff}d_g$ is the cross sectional area.

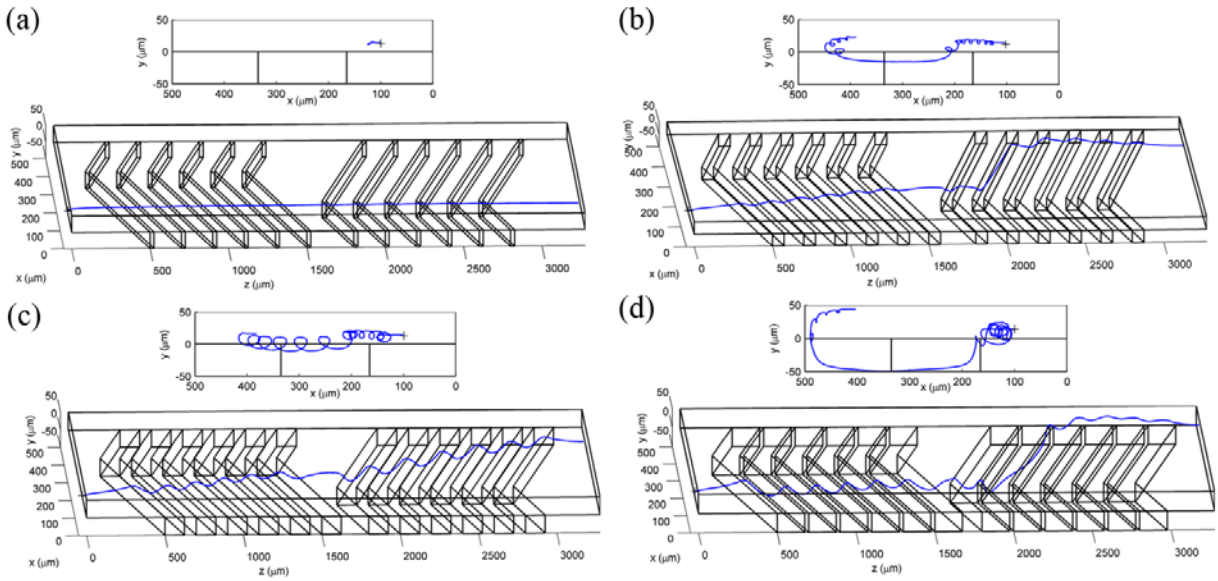

Fig. S9. Simulated streamline across the range of flow profile regimes for a 200 μm pitch with (a) 25 μm, (b) 75 μm, (c) 125 μm, and (d) 175 μm groove widths.

Fig. S9 demonstrates the flow regimes in the herringbone mixer as a function of increasing groove width. As the groove width increased, the hydraulic resistance within the groove decreased, diverting more flow into and deeper in the grooves. This explained the slight deflection of streamlines for small groove widths (Fig. S9(a)); increased deflection and improved surface contact, especially along the channel bottom (Fig. S9(b)) for increasing groove width; a helical pattern in and out of the grooves with transverse motion along the channel (Fig. S9(c)) as the resistances balance; and finally decreased interaction as the groove width increased further and enabled a significant portion of the fluid to completely enter and flow along the grooves (Fig. S9(d)).

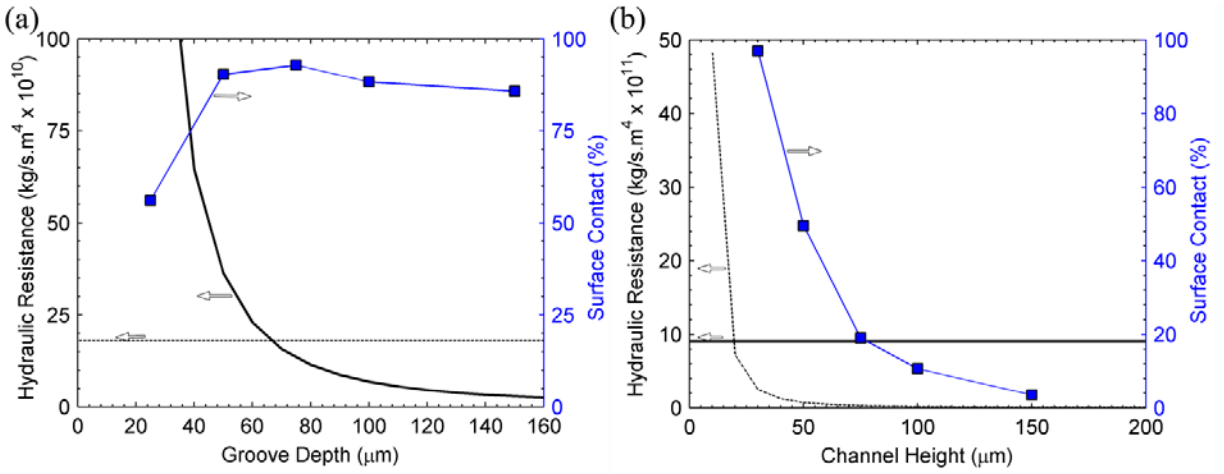

Fig. S10. Representative theoretical hydraulic resistance (left ordinate axis) of the channel (••••) and within the groove (—), plotted with the simulated total surface interaction (right ordinate axis (■)) for (a) a pitch of 200 μm, groove width of 125 μm, and channel height of 50 μm as a function of groove depth, and (b) a pitch of 100 μm, groove width of 50 μm, and groove depth of 50 μm as a function of channel height.

References

1. ESI Group CFD, 2010.0, Paris, France, 2010.
2. The MathWorks Inc., MATLAB Release 2010a, Natick, MA, 2010.
3. B. J. Kirby, *Micro- and Nanoscale Fluid Mechanics, Transport in Microfluidic Devices*, Cambridge University Press, Cambridge, 2010.